ORIGINAL RESEARCH

CT and MR Imaging Cochlear Distance Measurements May Predict Cochlear Implant Length Required for a 360° Insertion

S.E.J. Connor
D.J. Bell
R. O'Gorman
A. Fitzgerald-O'Connor

BACKGROUND AND PURPOSE: A preoperative prediction of the 360° point insertion depth would aid the planning of electric acoustic stimulation (EAS) implantation. The purpose of this study was to establish whether the distance between the round window and the opposite cochlear wall on CT or MR imaging may be used to predict the length of a cochlear implant electrode array required to be inserted to the 360° point of the basal turn.

MATERIALS AND METHODS: CT and MR imaging data were studied in 19 patients undergoing cochlear implantation. Distances were measured between the round window and the opposite outer cochlear wall on an oblique paracoronal reformatted image. Adjusted distance measurements were applied to a spiral function to estimate the length of an electrode array extending between the round window entry point and the 360° point. This was compared with measurements of implant length to this insertion depth on postoperative CT.

RESULTS: Intraobserver reproducibility for each of the 2 observers was $r = 0.85/0.55$ for CT and $r = 0.87/0.67$ for MR imaging. Interobserver reproducibility was $r = 0.68$ for CT and $r = 0.84$ for MR imaging. There was no bias between CT and MR imaging measurements, with a mean difference of less than 0.1 mm. CT and MR imaging estimates markedly correlated with the actual length of the electrode array extending to the 360° insertion depth (SD between the estimated and actual length was 0.84 mm for CT and 0.87 mm for MR imaging).

CONCLUSIONS: CT and MR imaging measures of cochlear distance (CD) were used to predict insertion depths to 360°, and these were markedly concordant with the actual length of the electrode array required to reach this point. MR imaging measurements were more precise and similar in accuracy to those obtained with CT.

During the past decade, combined electric acoustic stimulation (EAS) has been increasingly applied to patients with preserved low-frequency hearing[1-3] and to candidates for conventional cochlear implantation.[4,5] Limited insertions of the electrode array over 1 complete turn (to the 360° point) are used to minimize damage to the more apical cochlea and conserve residual hearing.[1-3,6] Several aspects will influence the insertion depth required to reach the 360° point of the basal turn, including the proximity of the array to the modiolus and the site of entry into cochlea. Although these factors may be somewhat controlled by surgical technique and choice of array, the dimensions of the cochlea may vary by 15% to 30%[7-9] and so may markedly and unpredictably influence the required insertion depth. Intraoperative fluoroscopy may allow real-time monitoring of the insertion depth angle[10]; however, there is an additional staffing, equipment, and radiation burden. A preoperative imaging study that is able to determine the optimum depth for EAS implant insertion would be of benefit.[6,11]

Optimal imaging protocols before cochlear implantation have not been well defined, with both CT and MR imaging being contributory.[12,13] MR imaging has some advantages in demonstrating the presence of the cochlear nerve, early labyrinthine fibrosis, and minor labyrinthine dysplasia without exposure to ionizing radiation,[14,15] so preoperative MR imaging alone has become an established practice in many implantation programs. The superior spatial resolution of CT would be expected to provide greater accuracy in demonstrating cochlear dimensions[8,16]; however, this has not been studied.

A previous report aimed at predicting the 360° point insertion depth used image-rendering software to optimally display the CT appearances of the basal turn of the cochlea, before manually placing 25 to 30 reference points along the lateral wall.[6] In an attempt to validate a more rapid, pragmatic method to predict the insertion depth angle, Escude et al[11] defined a simple measurement extending from the round window to the opposite wall of the basal turn through the midmodiolar axis. When applied to an equation derived from a spiral function, this cochlear distance (CD) was shown to correlate well with the radiographically demonstrated insertion depth angle of a perimodiolar array.[11]

The application of MR imaging protocols to the evaluation of cochlear dimensions and the reproducibility of cochlear measures has not been explored. We aimed to use the technique described by Escude et al[11] to address several issues:

1. To correlate the measurements of CD obtained with CT with those obtained with MR imaging.
2. To assess the precision (intraobserver and interobserver reproducibility) of CT and MR imaging CD measurements.
3. To determine whether CT or MR imaging measures of the

Received September 28, 2008; accepted after revision January 28, 2009.

From the Department of Radiology (S.E.J.C., D.J.B., R.O.), and Ear Nose and Throat Department and Auditory Implantation Centre (A.F.-O.), Guy's and St. Thomas' Hospital; and Departments of Neuroradiology (S.E.J.C.) and Medical Physics (R.O.), King's College Hospital, London, United Kingdom.

Please address correspondence to Dr. S.E.J. Connor, Neuroradiology Department, Ruskin Wing, Kings College Hospital, Denmark Hill, London, United Kingdom, SE5 9RS; e-mail: steve.connor@kch.nhs.uk

DOI 10.3174/ajnr.A1571

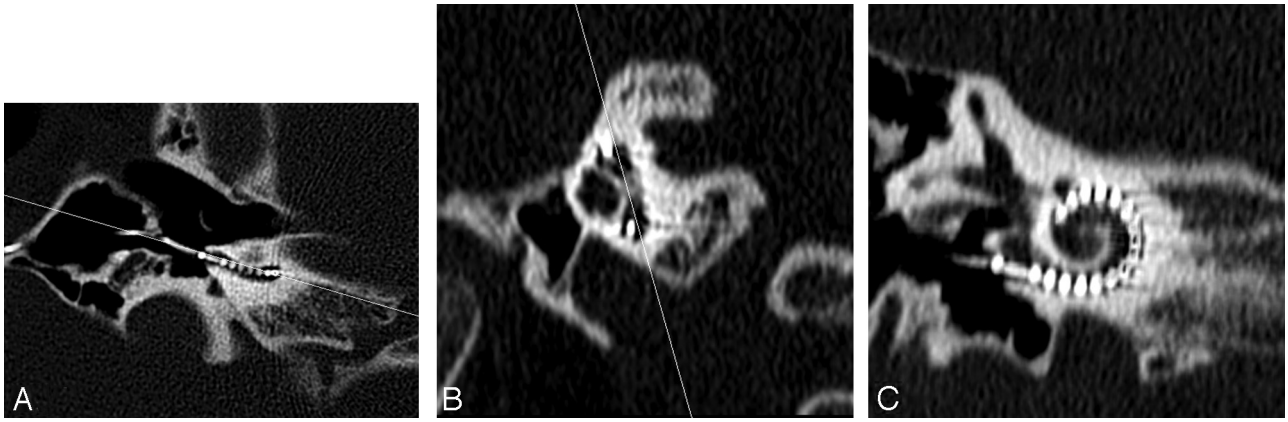

Fig 1. Axial CT image (*A*) through the inferior segment of the basal turn in a postimplant cochlea with a line shown angled to the basal turn. An oblique sagittal reformat (*B*) is obtained perpendicular to the line through the basal turn in (*A*). A line joining the midsuperior and -inferior segments of the basal turn in (*B*) is used to obtain the double oblique coronal reformat of the basal turn shown in (*C*).

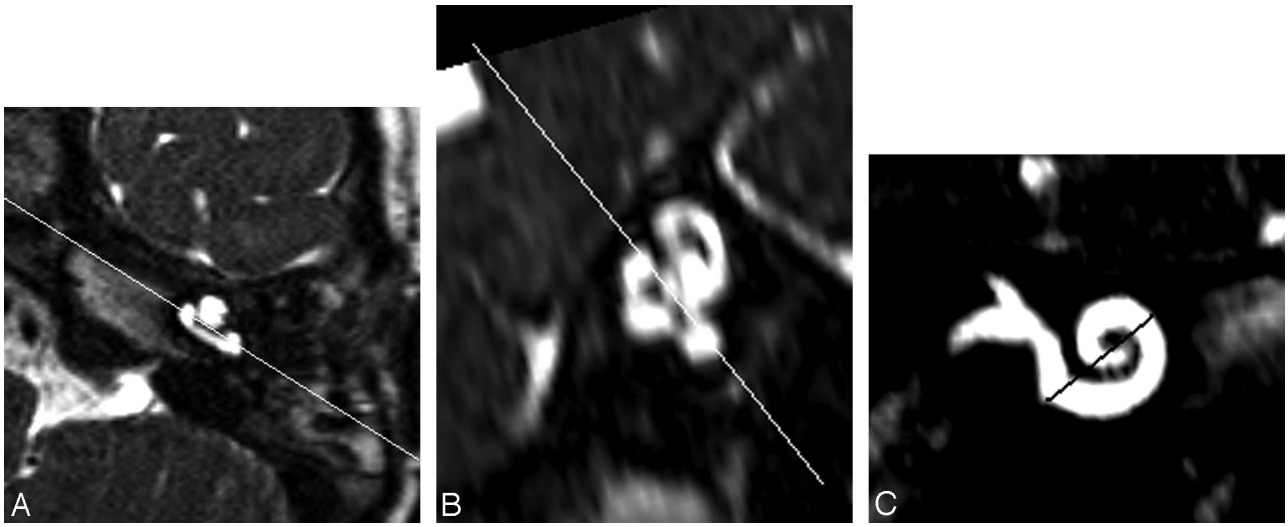

Fig 2. Axial 3D-DRIVE MR image (*A*) through the inferior segment of the basal turn in a preimplant cochlea with a line shown angled to the basal turn. An oblique sagittal reformat (*B*) is obtained perpendicular to the line through the basal turn in (*A*). A line joining the mid superior and inferior segments of the basal turn in (*B*) is used to obtain the double oblique coronal reformat of the basal turn shown in (*C*).

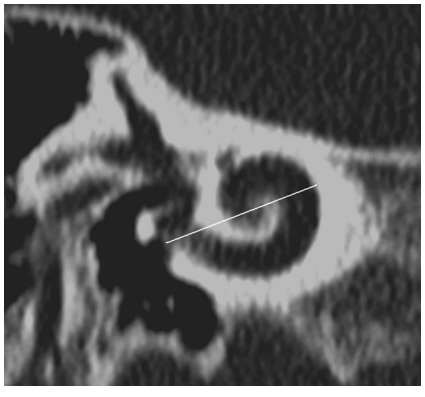

Fig 3. CD measurement is illustrated on a double oblique 1-mm thick reformatted CT through the basal turn of the cochlea. CD is measured from the midround window through the midmodiolar axis (confirmed by scrolling through adjacent images in this case) to the opposite wall of the basal turn. The midround window was identified on the reformatted MR imaging section by referring to an adjacent, more posterior image where the midinferior point of the round window "keyhole" could be extrapolated. The line indicating the CD measurement for MR imaging is shown in Fig 2*C*.

CD may accurately predict the length of a "straight" cochlear implant array extending between the midround window and the 360° point on a postoperative CT study.

Materials and Methods

CT temporal bone and MR imaging temporal bone data were obtained for 19 pediatric patients (9 girls, 10 boys; mean age, 6.8 years; age range, 2–17 years; SD, 4.4 years) who underwent cochlear implantation. Cochlear implantation was performed with a HiFocus 1j electrode (Advanced Bionics, Sylmar, Calif) "straight" array inserted through an extended round window approach. The study was reviewed by the local National Health Service Research Ethics Committee and was considered to represent "service evaluation." A total of 37 cochleas (including 20 implanted cochleas) were studied in 19 patients (1 nonimplanted cochlea was not included because of scan obliquity excluding it from the image volume). CT was performed with a Brilliance 40 scanner (Philips Medical Systems, Best, the Netherlands) with parameters of mA, 100; kV, 120; FOV, 180 mm; matrix, 768 × 768; pitch, 0.348; section thickness, 0.67 mm; and reconstruction index, 0.33 mm (voxels of 0.23 × 0.23 × 0.33 mm). MR imaging

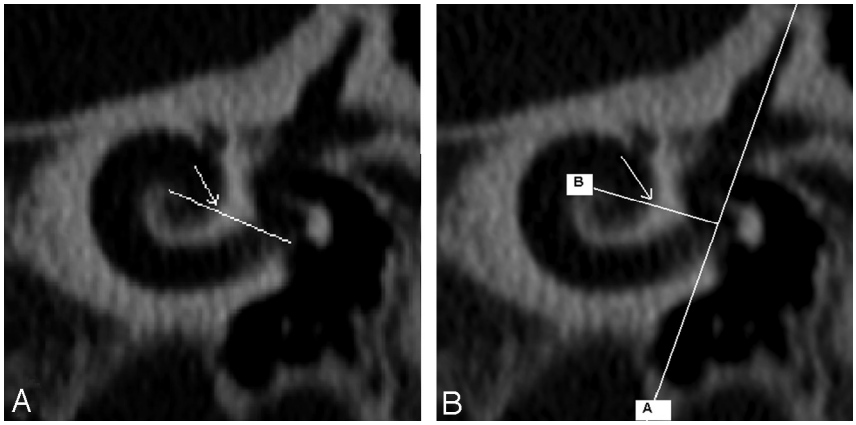

Fig 4. The distal reference (360° point) was defined in 2 ways according to Xu et al and Marsh et al, depending on where projected imaginary lines crossed the cochlear lumen [arrows in (*A*) and (*B*)]. For the Xu et al measurement (*A*), the imaginary line extended from the center of the cochlea to the midround window. For the Marsh et al measurement (*B*), the imaginary line B extended from the center of the cochlea to a perpendicular vertical line A through the superior semicircular canal and the vestibule.

was performed with an Intera 1.5T unit (Philips Medical Systems) T2 3D driven equilibrium sequence and parameters TR, 1500 ms; TE, 250 ms; echo-train length, 74; flip angle, 90°; FOV, 130 mm; 256 × 204 voxel matrix; NEX, 2; and section thickness, 1.4 mm, with 0.7-mm section spacing (voxels of 0.64 × 0.64 × 0.7 mm). MR imaging was performed before implantation, and CT was performed as part of routine clinical protocol after implantation for assessment of electrode position.

Image Analysis

The 3D data were reconstructed on an Extended Brilliance Workspace workstation (version 3.0.1.5000; Philips Medical Systems). For both the CT and MR imaging studies, a double-oblique paracoronal reformatted image was obtained (Figs 1 and 2). This was rendered with a 1-mm maximum intensity projection (MR imaging) or 1-mm thick reformat (CT). Thus, it was generally possible to visualize the basal turn from the round window to the opposite outer cochlear wall on a single image (Fig 3). CT was viewed with a window width/center of 4000/400, whereas MR imaging window settings were optimized to define the whole cochlea with the window width widened until a "penumbra" at the outer border of the basal turn started to appear.

The CD was measured from the midround window (with cross reference to orthogonal images as required), through the midmodiolar axis (confirmed by scrolling through adjacent images) to the opposite wall of the basal turn (Fig 3).[11] The distances were recorded to the nearest 0.1 mm for both imaging modalities. The measurements were recorded by 2 independent radiologist observers (observer A with 13 years of radiology experience, observer B with 5 years of radiology experience) who had previously reviewed 5 images together to ensure consistency. Each observer made 2 sets of measurements of each cochlea with an interval between measurements of more than 4 weeks.

For the implanted cochleas ($n = 20$), the length of electrode array extending between the round window entry point and the 360° point was documented on postoperative CT. Two lengths were calculated by scrolling through adjacent images, according to definitions of the 360° point by Xu et al[9] and Marsh et al[17] (Fig 4). The length was calculated by measuring the distance from the distal-most contact to the 360° point and the distance from the reference electrode to the wire at the midround window (Fig 5). If the electrode array extended beyond the 360° point, the distance was measured by counting the number of 1.1-mm gaps between electrode contacts (each "gap" was divided into quarters) distal to the 360° point. The distance between the reference electrode and the distal-most contact was 19 mm (manufacturer's information); thus, it was possible to calculate the length of the array extending through 1 complete turn to the 360° point (CALC 360).

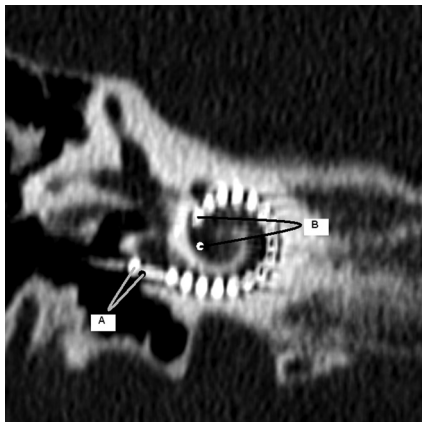

Fig 5. The CALC 360 was measured by use of the distance from the reference electrode to the wire at the midround window (A, black mark indicates midround window) and the distance from the distal-most contact to the 360° point (B, white mark indicates the 360° point as per Xu et al and as seen in Fig 4*A*).The distance between the reference electrode and the distal-most contact was 19 mm; thus, it was possible to calculate the length of the array extending through 1 complete turn to the 360° point (CALC 360).

Statistical Analysis

The precision (interobserver and intraobserver reproducibility) of CT and MR imaging measurements of the CD was determined by use of the Pearson linear correlation coefficient. Interobserver reproducibility (CT and MR imaging) was evaluated by use of the mean values of the 2 measurements obtained by each observer. Interobserver and intraobserver mean difference (SD) was also calculated.

CD measurements for CT vs MR imaging were compared by 1) use of the mean of measurements obtained by both observers (4 measures for each cochlea) and 2) use of the mean of measurements obtained by each observer (2 measures for each cochlea).

The mean difference (SD) of the measurements (MR CD−CT CD) was calculated, and the Pearson linear correlation coefficient was used to compare the CT with the MR imaging measurements (overall and for each observer).

A spiral function was used to estimate the insertion depth to the

Table 1: Intraobserver reproducibility (mean difference [SD] and Pearson linear correlation coefficient) for CT and MR imaging cochlear dimensions measurements

	Intraobserver Reproducibility (Observation 1-Observation 2) Mean Difference (SD) (mm)	Intraobserver Reproducibility (Pearson R)
CT (observer A/observer B)	−0.03 (0.21)/0.06 (0.33)	0.85/0.55
MRI (observer A/observer B)	−0.01 (0.23)/−0.04 (0.34)	0.87/0.67

Table 2: Interobserver reproducibility (mean difference [SD] and Pearson linear correlation coefficient) for CT and MR imaging cochlear dimensions measurements

	Interobserver Reproducibility (Observer A-Observer B) Mean Difference (SD) (mm)	Interobserver Reproducibility (Pearson R)
CT	−0.19 (0.28)	0.68
MRI	−0.16 (0.26)	0.83

360° point (EST 360) on the basis of the cochlear distance. The function models the line along the outer wall of the cochlea,[9,11] and when substituted with constants, it approximates to EST 360 = 2.62CD × $\log_e$ (1 + 360/235)[11] and can then be reduced to EST 360 = 2.434CD.

The accuracy of CT and MR imaging EST 360 to predict the length of electrode array extending between the round window entry point and the 360° point (CALC 360) was determined 1) by use of the mean of measurements obtained by both observers (the 4 measures for each cochlea) and 2) by use of the mean of measurements obtained by each observer (the 2 measures for each cochlea) for both CT and MR imaging.

The CD was initially adjusted by subtracting an "offset" of 1 mm to account for the array lying slightly toward the modiolus from the outer scala tympani wall.[6] The EST 360 was subtracted from the CALC 360, and mean/SD was calculated. The Pearson linear correlation coefficient was again used to assess the accuracy of the CT and MR imaging CD measurements to predict the CALC 360. The ideal "offset" was then calculated so that the mean EST 360 equalled the mean CALC 360.

Results

The CD with use of the mean of measurements obtained by both observers (4 measures for each cochlea) on the CT studies was mean (SD) 9.36 (0.31) mm (range, 8.3–10.4 mm). When analyzed by side, there was little difference with mean 9.32 (0.31) mm on the left and 9.39 (0.32) mm on the right.

Intraobserver reproducibility (CT/MR imaging) for each of the 2 observers and interobserver reproducibility (CT/MR imaging) are shown in Tables 1 and 2. Mean difference and SD of the observations were within the voxel resolution for MR imaging. The intraobserver differences were not significant, but the interobserver differences were significant on a Student paired *t* test ($P < .05$).

There was no bias between CT and MR imaging measurements, with a mean difference of less than 0.1 mm. There was a high degree of correlation for CT/MR imaging measures achieved by observer A (Table 3).

When applied to the modified spiral function, the overall CT and MR imaging measures (EST 360) moderately correlated with the CALC 360 for the Marsh et al[17] definition and markedly correlated with the CALC 360 for the Xu et al[9] definition (Table 4). In each case, the mean EST 360 was longer

Table 3: Comparison of CT and MR imaging cochlear dimension measurements (mean difference [SD] and Pearson linear correlation coefficient)

	Mean (SD) Difference (MR Imaging−CT)	Pearson *r*
A	0.044 (0.19) mm	0.8
B	0.023 (0.33) mm	0.4
A+B	0.07 (0.19) mm	0.75

than the mean CALC 360. The mean difference and SD between the estimated and actual length (CALC 360−EST 360) was −1.1 ± 0.84 mm for CT and −1.0 ± 0.87 mm for MR imaging for the Xu et al[9] definition. To optimize the relationship between EST 360 and CALC 360 so that there was no mean difference, the CD could be corrected by an "offset" to account for the array lying toward the modiolus from the outer cochlear wall. This was calculated to be 1.4 mm (0.7 mm from each wall) to approximate the Xu et al[9] CALC 360 and 1.7 mm (0.85 mm from each wall) to approximate the Marsh et al[17] CALC 360.

Discussion

MR imaging has a major role in the preoperative assessment of patients undergoing cochlear implantation, and it has advantages vs CT in the detection of important abnormalities such as cochlear nerve aplasia or cochlear fibrosis.[14,15] Because there is no ionizing radiation burden, MR imaging is particularly favored in the pediatric population.

In addition to its role in selecting appropriate candidates, imaging may help guide the implantation technique. The ability of CT to predict the length of cochlear array required to attain a particular insertion depth has been explored.[6,11] Although MR imaging has been applied to the measurement of distances in the jaw bones,[18] its accuracy has not been assessed in the context of cochlear measurements. The superior spatial resolution of CT would be expected to aid the depiction of CDs. The CT voxel size was 0.23 × 0.23 × 0.33 mm vs the MR imaging voxel size of 0.64 × 0.64 × 0.7 mm in our study. MR imaging spatial distortion is bandwidth dependent and may result from susceptibility and chemical shift effects. Despite the high contrast between cochlear fluid and cortical bone achieved with the 3D DRIVE sequence,[19] the interface was generally less clear compared with CT, and its definition required a judicious choice of windowing parameters. Although there were potential difficulties in defining the CD on the CT images of postimplant cochleas because of fluid in the round window and artifacts from electrode contacts, the similar reproducibility and superior accuracy achieved with implanted vs nonimplanted CT measurements would indicate that this was not detrimental to image evaluation. The thicker-section coronal oblique reformats and smoothing algorithms of the reconstruction software required for the measurement of CDs would limit spatial resolution, but this would be applicable to both CT and MR imaging. When considering these factors, it is somewhat surprising that MR imaging measurements were more precise and similar in accuracy to those obtained with CT.

The definition of the limits of CALC 360 was based on those used in previous CT and radiographic studies. The distal reference (360° point) was defined in 2 ways according to Xu et

Table 4: Comparison of EST 360 vs CALC 360 for Xu et al[9] and Marsh et al[17] methods (mean difference [SD], range, and Pearson linear correlation coefficient)

	Xu et al[9]		Marsh et al[17]	
	Mean difference (SD) (and range): CALC 360 − EST 360	Pearson *r*	Mean difference (SD) (and range): CALC 360 − EST 360	Pearson *r*
CT				
A	−0.79 (0.84) mm (−0.54–2.4)	0.67	−1.49 (1.04) mm (−1.6–2.9)	0.62
B	−1.36 (0.90) mm (−0.43–2.9)	0.49	−2.05 (1.13) mm (−1.6–3.7)	0.47
A+B	−1.06 (0.84) mm (−0.80–2.2)	0.61	−1.75 (1.09) mm (−1.6–3.2)	0.53
MR Imaging				
A	−0.76 (0.81) mm (−0.70–2.3)	0.75	−1.45 (1.15) mm (−1.9–3.1)	0.57
B	−1.30 (1.05) mm (−0.70–3.4)	0.52	−1.98 (1.29) mm (−1.9–3.7)	0.43
A+B	−1.0 (0.87) mm (−0.70–2.9)	0.67	−1.72 (1.17) mm (−1.9–3.4)	0.52

Note:—EST 360 indicates an estimate of the insertion depth to the 360° point based on the cochlear distance measured; CALC 360, calculation of the length of the array extending through 1 complete turn to the 360° point on postoperative CT.

al[9] and Marsh et al,[17] depending on where projected imaginary lines crossed the cochlear lumen. In the case of Xu et al,[9] the imaginary line extended from the center of the cochlea to the midround window. For the Marsh et al[17] measurement, the imaginary line extended from the center of the cochlea to a perpendicular vertical line through the superior semicircular canal and the vestibule. The 360° point according to Xu et al[9] was more distal to that defined by Marsh et al[17] and corresponded better with the EST 360 with use of the a priori "offset" of 1 mm. The point at which the electrode array passed closest to the midround window was used as the proximal reference point because the study was designed for patients by use of round window cochlear implant insertions. A slightly greater SD of the difference between EST 360 and CALC 360 for the Marsh et al[17] definition was noted. This may have been the result of a greater error in the measurement of CALC 360 because the orientation of the electrode contacts is in the z-axis (with poorer spatial resolution) at this more proximal point and is, hence, associated with greater "blurring." The inherent scan resolution was generally sufficient to visualize the individual electrode contacts and measure CALC 360 relative to the apical electrode array, despite beam-hardening artifacts and a restricted Hounsfield unit range. It is appreciated that there are potential errors in electrode contact localization, and the results should be interpreted in the context of potential inaccuracies (range, 0.03–0.2 mm) recently demonstrated by 64-section CT scanners.[20]

Our study did not attempt to correlate the CD with direct measures of basal cochlear length but, rather, with the more pragmatic issue of the length of a "straight" electrode required to extend to the 360° point. It was observed that the proximal array was not closely applied to the floor of the inferior segment of the basal turn, and it was only when it encountered the ascending segment that it tended to lie along the outer aspect of the cochlea. The proximity to the outer aspect of the cochlea and the degree of scala crossover may also be influenced by kinking or friction at the distal aspect of the cochlear array so this may also influence the depth of the attempted insertion. It is clear that these factors affect the CALC 360 and, hence, the degree of "offset" subtracted from the CD. It would also be useful to explore the influence of other factors such as the use of EAS electrode arrays, cochleostomy approach, and change in spiral morphology (eg, in cochlear dysplasia) on the "offset" correction factor.

It could be argued that preoperative imaging should be used to custom fit the electrode insertion depth to satisfy pitch placement according to the Greenwood frequency map, which would not necessarily entail a 360° insertion. However, early experience in EAS has shown that some patients were offered the option of a program that included an auditory-electrical crossover region, actually preferred it, and happily used auditory and electrical stimulation at the same frequency. The more important factor seems to be that when implant depth is greater than 360°, then a marked loss of residual hearing is seen; hence, this insertion depth was our main focus.

The CD measurements in our series of pediatric cochleas were similar (mean, 9.36 mm; SD, 0.31 mm; range, 2.1 mm) to those documented previously in a mixed pediatric and adult population (mean, 9.23 mm; SD 0.53 mm; range, 2.9 mm).[11] Our data equate to a mean (SD) length of the lateral wall of the cochlea from the round window to the 360° point of 22.6 mm (0.7 mm). The accuracy of EST 360 in the prediction of CALC 360, with SD of the difference being 0.84 mm (CT) and 0.87 mm (MR imaging), should be interpreted in the context of an overall range in cochlear length of 5.1 mm. We intend to apply our data to the planning of EAS implants, where it is important that the insertion depth does not exceed 360°. Inserting a straight array to no more than EST 360−2 SD of the difference between EST 360 and CALC 360 (approximately 1.7 mm for the Xu et al[9] point) would seem appropriate.

Conclusions

We describe a rapid, pragmatic method that can be applied to routine cochlear implantation preoperative imaging, to estimate the length of a straight array required to reach an insertion depth of 360°. The depiction of distances on MR imaging was reproducible within the voxel resolution of the images, and they did not significantly differ from those obtained with CT. The SD of the difference between EST 360 and CALC 360 may be applied to the EST 360 to select the length of a straight electrode array insertion, which is unlikely to exceed the 360° point.

References

1. Kiefer J, Pok M, Adunka O, et al. **Combined electric and acoustic stimulation of the auditory system: results of a clinical study.** *Audiol Neurootol* 2005; 10: 134–44
2. Gstoettner WK, Helbig S, Maier N, et al. **Ipsilateral electric acoustic stimulation of the auditory system: results of long term hearing preservation**. *Audiol Neurootol* 2006;11 Suppl 1:49–56
3. Gstoettner W, Kiefer J, Baumgartner WD, et al. **Hearing preservation in co-**

chlear implantation for electric acoustic stimulation. *Acta Otolaryngol* 2004;124:348–52
4. Fraysse B, Macias AR, Sterkers O, et al. **Residual hearing conservation and electroacoustic stimulation with the nucleus 24 contour advance cochlear implant.** *Otol Neurootol* 2006;27:624–33
5. James CJ, Fraysse B, Deguine O, et al. **Combined electroacoustic stimulation in conventional candidates for cochlear implantation.** *Audiol Neurootol* 2006;11 Suppl 1:57–62
6. Adunka O, Unkelbach MH, Mack MG, et al. **Predicting basal cochlear length for electric-acoustic stimulation.** *Arch Otolaryngol Head Neck Surg* 2005;131: 488–92
7. Dimopoulos P, Muren C. **Anatomic variations of the cochlea and relations to other temporal bone structures.** *Acta Radiol* 1990;31:439–44
8. Ketten DR, Skinner MW, Wang G, et al. **In vivo measures of cochlear length and insertion depth of nucleus cochlear implant electrode arrays.** *Ann Otol Rhinol Laryngol Suppl* 1998;175:1–16
9. Xu J, Xu S-A, Cohen LT, et al. **Cochlear view: postoperative radiography for cochlear implantation.** *Am J Otol* 2000;21:49–56
10. Fishman AJ, Roland JT Jr, Alexiades G, et al. **Fluoroscopically assisted cochlear implantation.** *Otol Neurootol* 2003;24:882–86
11. Escude B, James J, Deguine O, et al. **The size of the cochlea and predictions of insertion depth angles for cochlear implant electrodes.** *Audiol Neurootol* 2006;11:27–33
12. Gleeson TG, Lacy PD, Bresnihan M, et al. **High resolution computed tomography and magnetic resonance imaging in the preoperative assessment of cochlear implant patients.** *J Laryngol Otol* 2003;117:692–95
13. Trimble K, Blaser S, James AL, et al. **Computed tomography and/or MRI before paediatric cochlear implantation. Developing an investigative strategy.** *Otol Neurootol* 2007;28:317–24
14. Ellul S, Shelton C, Davidson HC, et al. **Preoperative cochlear implant imaging: is magnetic resonance imaging enough?** *Am J Otol* 2000;21:528–33
15. Parry DA, Booth T, Roland PS. **Advantages of magnetic resonance imaging over computed tomography in preoperative evaluation of pediatric cochlear implant candidates.** *Otol Neurootol* 2005;26:976–82
16. Skinner MW, Ketten DR, Holden LK, et al. **CT-derived estimation of cochlear morphology and electrode array position in relation to word recognition in Nucleus-22 recipients.** *J Assoc Res Otolaryngol* 2002;3:332–50
17. Marsh MA, Xu J, Blamey PJ, et al. **Radiologic evaluation of multichannel intracochlear implant insertion depth.** *Am J Otol* 1993;14:386–91
18. Nael CJ, Pretterlieber M, Gahleitner A, et al. **Osteometry of the mandible performed using dental MR imaging.** *AJNR Am J Neuroradiol* 1999;20: 1221–27
19. Jung NY, Moon W-J, Lee MH, et al. **Magnetic resonance cisternography: comparison between 3-dimensional driven equilibrium with sensitivity encoding and 3-dimensional balanced fast-field echo sequences with sensitivity encoding.** *J Comput Assist Tomogr* 2007;31:588–91
20. Verbist BM, Joemai RM, Teeuwisse WM, et al. **Evaluation of 4 multisection CT systems in postoperative imaging of a cochlear implant: a human cadaver and phantom study.** *AJNR Am J Neuroradiol* 2008;29:1382–88